ENGINE – **EN**hanced **G**eothermal **I**nnovative **N**etwork for **E**urope
Workshop 3, "Stimulation of reservoir and microseismicity"
Kartause Ittingen, Zürich, June 29 – July 1, 2006, Switzerland

Micro-Seismic Interpretation of Hydraulic Fracture Treatments

C.J. de Pater, N.R. Warpinski and L.G. Griffin
Pinnacle Technologies
Kalfjeslaan 54
2654AJ Delft, The Netherlands
e-mail: hansp@pinntech.nl

Abstract

For completing wells in oil and gas reservoirs it is quite common to stimulate the well with a hydraulic fracture. However, the treatment is often sub-optimal because the fracture geometry is poorly known. Recent advances in micro-seismic monitoring have aided in optimizing hydraulic fractures and revealed that fracture geometry often deviates from simple modeling.

For accurate event location we need first to establish a velocity model and we will show how this can be improved by a checkshot and using initial events. Furthermore we will discuss the application in a few field cases with unexpected fracture geometry. Characterization of fracture height growth, connection with faults and complex branched fractures will be shown as examples of micro-seismic monitoring. The material in this presentation was taken from the papers by Warpinski et. al. (2003) and Griffin et. al. (2003).

1. Introduction

Micro-seismic imaging of fluid injection and fracturing has been pioneered in the geothermal industry. For petroleum applications, micro-seismic monitoring has become commercially available in the last decade both for reservoir monitoring and hydraulic fracture mapping. In this paper we will show a significant improvement of the location accuracy by measuring the velocity structure of the reservoir and overburden layers. A few examples will be shown of complex fracture behaviour in stimulation injections. Interaction with natural fractures and faults yields sometimes an unexpected fracture geometry. In that sense there is also a link with the first observations of geothermal stimulations (Murphy, 1986). Increasing the surface area of the fracture system is beneficial for HDR stimulation and the same applies to stimulation of very tight gas reservoirs. In many cases, however, interaction with faults hampers effective stimulation because it is difficult to pump high concentration slurry through a fracture network with width restrictions. It is likely that interaction with faults is rather common but routine treatments have only pressure measurements and then it is impossible to detect fluid channeling along faults as we will show.

2. Micro-seismic mapping: Location Error and Velocity Model

The location of seismic events can be accomplished by observing an event on a string of geophones and modeling the arrival times with a forward model of all the travel paths. In that way, the source location can be determined from a match between model and measurement. In addition, the phase information on the triaxial geophones can be used to determine the direction from which the waves came. Using both P and S-waves yields additional information on the source location in the inversion.

The effect of the velocity structure on the error in the locations can be illustrated with a simple case of a symmetrical, three layer system. We assume that the reservoir layer has typical sandstone compressional and shear velocities of 4500 m/sec and 3,000 m/sec, respectively, and that the bounding layers have a lower velocity of V_P and V_S of 3500 ft/sec and 2000 m/sec, respectively. For this example the ratio of the velocities is the same for both P and S waves. The best case has the array straddled over the reservoir.

The top plot of Figure 1 shows the ray paths from the microseism to each receiver. The ray paths are extremely bent by the velocity variations. The bottom plot of Figure 1 shows the locations for a constant velocity throughout the region. In one case the velocity is for the fast layer (high velocity), another is for the slow layers (low velocity), and a third is for a RMS average of both velocities. The location is found using regression on the arrival times and using a grid search approach. Both methods give the correct answer for correct velocity information, but that can be quite different depending on the error in the velocity model. The example shows that if the velocity structure is not taken into account, the distances to the event can be in error by more than 25% of the distance to the event. Because the array is centered,

however, the elevations of the events will be relatively accurate (not the case if the shale velocities are different). A worse result is obtained when the array is located above the reservoir, such as would occur if the array was placed in an older well where perforations were isolated with a bridge plug.

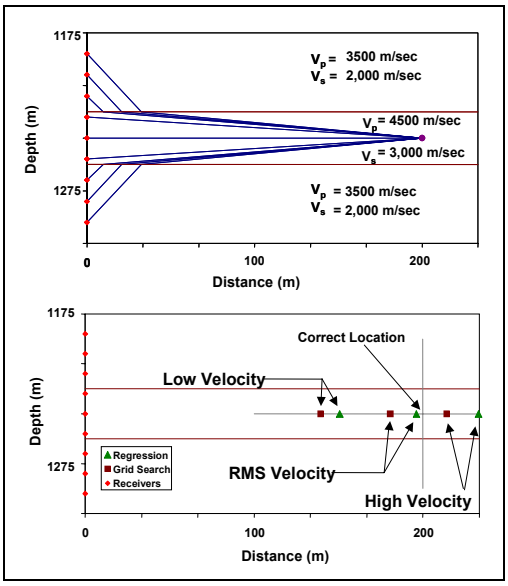

Figure 1: *Velocity-structure example for centered array.*

2.1 Formation Velocity Data

Formation velocity data can be obtained in a number of ways, but accuracy of measurement is a critical issue. Clearly, the most favorable approach is to perform a cross-well survey in order to develop P and S tomograms of the interval being studied, but even this approach is often limited to a single cross-section (lacking azimuthal information) and tomograms are seldom available for use in microseismic analysis.

In most cases the velocity is obtained from a dipole-sonic log. These logs provide high resolution of the velocity structure, but there is considerable potential for discrepancies. Most important, the measured (vertical) velocity represents the formation near the well. This may be different from the (horizontal) velocity farther from the well. A recent new development is to use VSP survey data (preferably in 3D) and combine the obtained velocity structure with the micro-seismic interpretation (Le Calvez *et. al.*, 2005). However, this is rather costly and can only be performed when there is an independent application of the VSP. Moreover, it still measures the vertical velocity.

Another approach is to jointly invert the microseismic data for both location and

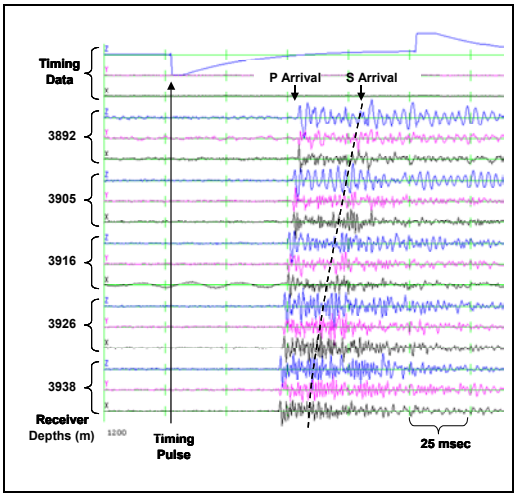

Figure 2: Example data set from perforation with trigger pulse on zero level.

formation velocities. However, in petroleum applications we usually are limited to small arrays of 8-12 receivers in one or two boreholes. Systematic errors are likely to result in large inaccuracies in such cases.

A practical solution has been to use the perforation or string shot that is routinely monitored for determining the orientation of the receiver as a timed source for extracting velocity data across wells. Although we have only limited data (a few ray paths) we can determine the velocity when we assume a layered earth model. In addition we can use the velocity to calibrate more detailed sonic logs

2.2 Perforation Timing Measurements

Perforation timing measurements for velocity extraction can be made if the time that we know accurately when the perforation is fired, the arrival time at the receivers and the distance between the wells. This method has been tried by other workers, but suffered from inaccuracy in the timing of the exact perforation explosion. We have carefully investigated the sequence of events and developed an accurate electronic system for picking up the time of the perforation shot.

Data analysis results in the determination of the trigger time, the P-wave arrival times at each receiver, and the S-wave arrival times (where available) at each receiver. With perforations and string shots, the P waves are usually quite good and can be accurately detected. Often the S waves may be a problem, as these sources are not particularly good S-wave generators. However, there are almost always some levels on which S waves can be detected. If S-waves cannot be picked

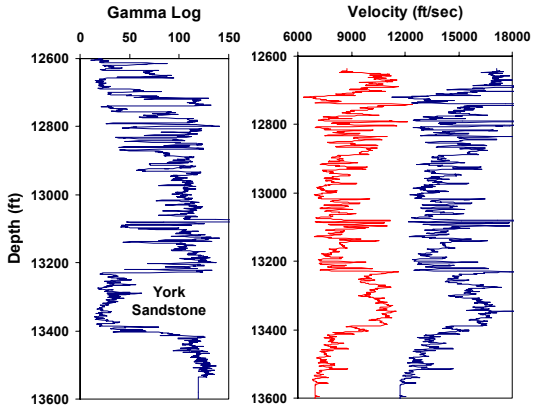

Figure 3: Dipole sonic log of Bossier interval in example well.

clearly, we use a quick and dirty solution: we determine the S-wave velocity from the first events in a fracture injection since these will be located near the well and given this location we can determine the velocity.

In addition to the timing data, the distance between the source and each receiver must be accurately known. Accurate distance measurements require both a surface survey (or GPS measurement) and deviation surveys for both wells.

3. Example 1: Bossier Play

The current Bossier play is located on the western flank of the East Texas Basin. Bossier wells generally produce dry gas with little or no water production from sands embedded in the Bossier, an Upper Jurassic marine shale. Productive sands are found at depths ranging from 12,000 to 15,000 feet. Several sands are targeted in this formation, but we will show only results for the York and Bonner sands. The sand porosities generally are in the 8 to 20% range, and can have a permeability of several millidarcies, but are normally less than 0.1 mD. All producing wells in the Bossier play need hydraulic fracturing. The development of optimal fracturing procedures, therefore, has a big impact on the long-term economic viability of the play.

3.1 Velocity Measurement for Bossier Monitoring

Microseismic monitoring of hydraulic fractures in the Bossier sands is operationally difficult because of the depth and high temperature, and analysis is complicated by the complexity of the reservoirs. Figure 3 shows an example dipole sonic log run in one of the test wells in

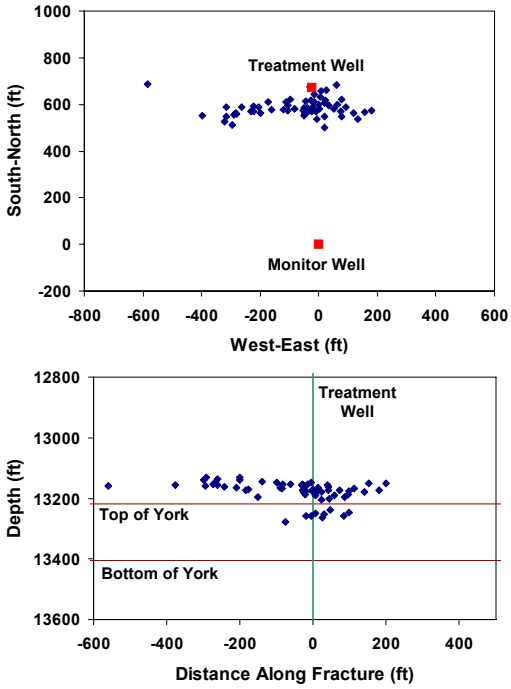

Figure 4. Microseismic locations using 3-layer velocity structure from dipole sonic log.

this Bossier monitoring program. Compressional-wave velocities vary from about 12,000 ft/sec to 17,000 ft/sec in the interval of interest and shear-wave velocities vary from 7,000 ft/sec to 11,000 ft/sec, based on this log. However, other sands may be present above the York sandstone in nearby offset wells, suggesting that the reservoir sizes are on the order of the well spacing.

For the first fracture treatment that was monitored in the Bossier, a limited number of high quality microseisms were selected to study velocity effects. These events were all located near or in the York sandstone. Using an initial 3-layer velocity model taken from the dipole sonic log, the maps shown in Figure 4 were obtained. As can be seen in this map, the resultant locations all appear to be too high (start well above the perforations) and too close (do not pass through the treatment well). An attempt was made to add additional layers to the velocity model, but the results did not improve significantly with even eight or ten layers.

Perforation timing measurements were performed in the treatment well as part of a three-treatment monitoring program and these data were used to calibrate the velocity structure. Only a five-level system was used because of operational constraints (a full 12-level system was used for the microseismic

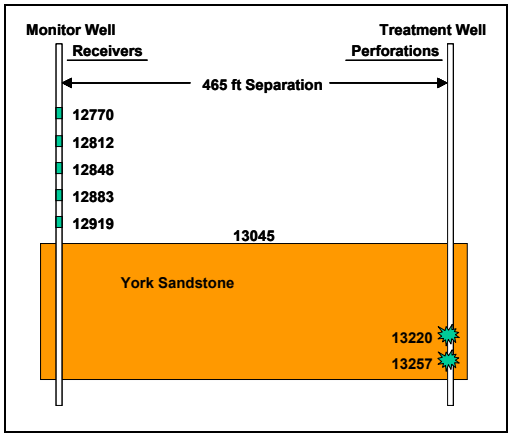

Figure 5: Schematic layout for Bossier perforation-timing measurement.

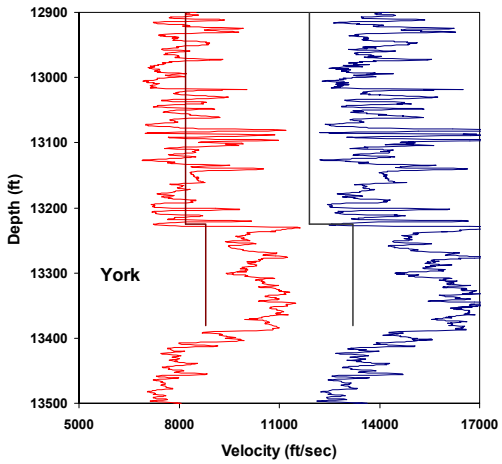

Figure 6: Velocity comparison for Bossier test.

monitoring), but two separate perforation runs were conducted, as shown schematically in Figure 5. These shots gave reasonable P-wave arrivals on all levels, but only provided clear S-wave data on a few levels of each test. From these data, it was deduced that the best-fit P-wave velocity for the York sandstone is 13,200 ft/sec and for the layers above it is about 11,900 ft/sec. For the S-wave velocities, 8,800 ft/sec and 8,200 ft/sec were determined to be appropriate velocities. A comparison is shown in Figure 6. These velocities are much different than what was obtained using the dipole sonic, but they may reflect the variability of anisotropy and sedimentary layers rather than any error in dipole-sonic measurement.

Using these perforation-timing results, the maps shown in Figure 7 were obtained. These results now start in the correct layer and pass through the treatment well, which makes the locations look much more probable. Similar behavior was observed for all three tests in this program with much more consistent locations determined using these lowered velocities. More detail was added to the velocity structure for tests having events at shallower depths, but all York and Bonner sandstone locations traversed this corrected velocity profile.

There are several potential causes for the observed discrepancy between the sonic and check-shot velocity, such as errors in the timing and distance measurement between wells. However, we see that we get a more consistent location interpretation when we use the check-shot velocity and this supports the accuracy of the perforation timing. This is generally the case when such measurements are obtained and, thus, performing perforation-timing measurements is now almost standard practice in microseismic monitoring. For most surveys we have conducted we found it critical to use the check-shot data to achieve an accurate micro-seismic event location.

3.2 APC Anderson #2 Fracture Treatment

The Bonner sand was perforated and a diagnostic injection and mini frac were conducted. Following a small acid injection the main hybrid frac was pumped in the Bonner. The injections were monitored with

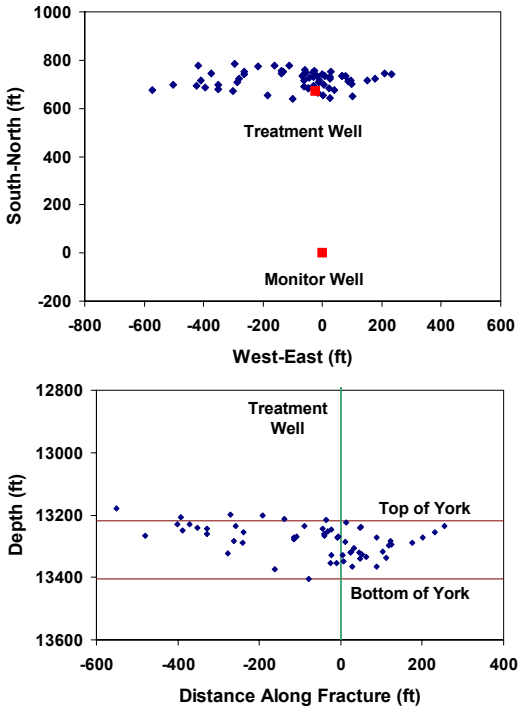

Figure 7: Microseismic locations using 3-layer velocity structure from perforation timing.

microseismic tools.

Figure 8 is a plot of the data collected on the Bonner stage. The 53 net feet of pay in the Bonner called for a smaller job, designed at 175,000 lbs of 20/40 proppant. We used a 35# borate gel in the crosslinked stages and the net pressure gain was over 1000 psi. Most of the net pressure rise in this treatment comes almost immediately after proppant arrives on formation, indicating a possible near-wellbore width restriction in the fracture. The relatively steep pressure increase and the instantaneous reaction to proppant indicate that this is not a tip screen-out. With the risk of a screenout with bottomhole gauges in the hole, it was decided to call flush early placing only 135,000 lbs of the designed 175,000 lbs into the created fracture.

In addition to fluid leaking off via localized faulting, the low efficiency of these jobs can also be attributed to a strong pressure dependant permeability effect in the bossier sands.

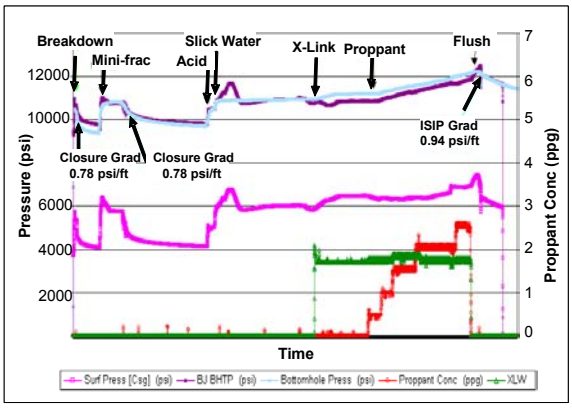

Figure 8: Fracture treatment in the Bossier formation, Bonner sand

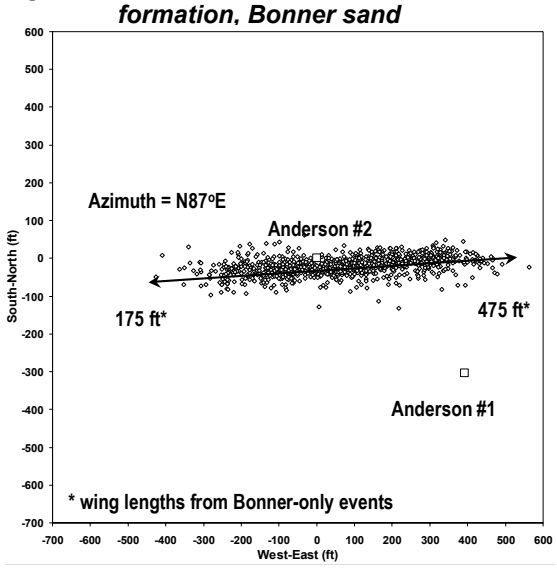

Figure 9: APC Anderson #2 Bonner Stimulation, Microseismic Data Plan View

3.3 Fracture Diagnostics (APC Anderson #2 Well)

Various direct and indirect fracture diagnostics were used to monitor the fracture treatments including:

- Microseismic imaging (for length, height and azimuth)
- Radioactive tagging with multiple isotopes (for near-wellbore height)
- Recording of bottomhole treatment pressure (to improve fracture simulation)
- Production logs (to evaluate effective propped fracture length and zonal coverage)

This project utilized a single microseismic imaging well to monitor the APC Anderson #2 Bonner treatments. The observation well was located 495 feet from the treatment well. Since microseisms are extremely small, a sensitive and high rate telemetry system is required to obtain accurate results. To meet these requirements, a twelve level, three-component retrievable geophone array was deployed using a fiber optic wireline unit. Once at depth, the receivers were clamped against the wellbore using mechanical arms. The tool string was configured for an aperture to adequately cover the target zones. The treatments were continuously monitored giving the capability of determining how the fractures grew with time, which proved critical for understanding the complex fracture growth.

The Bonner stimulation mapping results are shown in Figure 9 and Figure 10. The Bonner fracture also grew East/West with an azimuth of N87°E. The fracture growth was

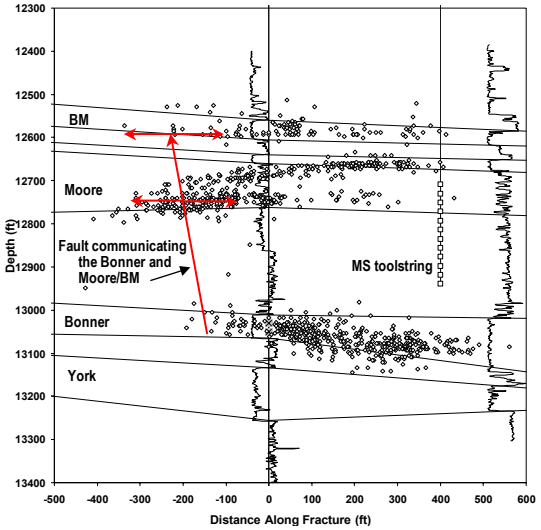

Figure 10: APC Anderson #2 Bonner Stimulation, Microseismic Data Side View

asymmetrical with an east wing extending 475 feet and a west wing of 175 feet. The Bonner treatment was also observed to have communicated upward in to the Moore and Bossier Marker sands through a fault. For the Bonner stimulation a significant amount of the treatment appears to have gone out of zone.

For the Bonner stimulation, the fault closest to the wellbore was open during the stimulation and is responsible for the upward communication to the Moore and Bossier Marker sands. Interestingly, this is the same fault that was observed to be non-communicating during a previous stimulation. The westward growth of the fracture in the Bonner sand appears to have been arrested where it intersected the fault. The fracture in the Bonner does not extend to the second fault observed during the York stimulation.

Results from the tracer log do not appear to be entirely consistent with the microseismic data. This, however, is not uncommon as the tracer logs only reflect the fracture geometry very close to the wellbore.

A retrievable pressure gauge was placed at the bottom of the well to record the bottomhole treating pressure during the treatment. The gauge recorded the data and was recovered after the treatment. This data was used to help calibrate the hydraulic fracture model for both sands.

4. Example 2: Waterfrac

The Barnett Shale is currently one of the most prolific gas reservoirs in the United States. The Barnett shale within the Fort Worth basin ranges from 200 to 800 ft in thickness and is approximately 500 ft thick in the core area of the field. The productive formation is typically described as a black, organic-rich shale composed of fine-grained, nonsiliciclastic rocks with extremely low permeability, ranging from 0.00007 to 0.005 md. The formation is abnormally pressured, and hydraulic-fracture treatments are necessary for commercial production because of the low permeability.

There has been a rebirth of drilling and refracturing activity in recent years because of the success of waterfracture, or "light-sand," fracturing treatments. This extremely low-permeability reservoir benefits from fracture treatments that establish long and wide fracture "fairways," which result in connecting very large surface areas of the formation with an extremely complex fracture network.

Similarly to HDR stimulation, it has been realized that production benefits from a large fracture area because the gas can only be recovered from the rock adjacent to the fracture surface. The fracture conductivity does not need to be very high and the fracture area can be enhanced by injecting large volumes of water. Only a little sand is added to ensure sufficient conductivity.

Figure 11 shows a typical example of fracturing in the Barnett; the long axis of the fracture network or "fairway" (oriented ~N40E in the core area of the Fort Worth Basin) is referred to as the hydraulic fracture "fairway length" while the short axis of the rectangle (from NW to SE) is typically referred to as "fairway width". For vertical wells, these fairway dimensions can approach about 4000 ft in length and up to 1200 ft in width. Figure 11 shows a typical fracture fairway network from a vertical well in the core area of the Barnett. The microseismic events are shown as points on this plan view and the gross fracture area is immediately obvious. The points can be analyzed with time and a linear regression algorithm applied to identify events that happen sequentially and appear to be related to a specific fracture structure. These sequential linear structures are highlighted with lines representing the minimum number and size of likely fracture segments.

This well's fracture length is more than 4000 ft long (2000 ft half-lengths) and "fairway" width is about 1000 ft across. The individual fracture structures are shown as line segments on the map; total fracture network length on this treatment was estimated as 30,000 ft. The five small squares seen just outside the fracture network show the locations of wells that were temporarily killed by the frac treatment on this well, confirming that the fracture network indeed extended as far as the

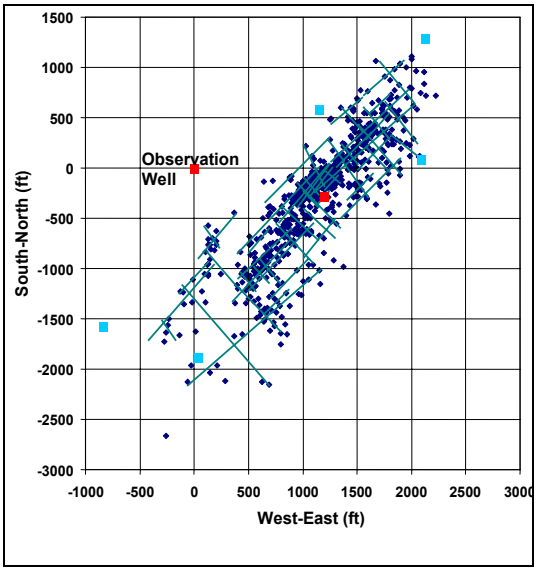

Figure 11: Plan view of microseismic map, showing a large waterfrac with extremely long and complicated fracture growth.

micro-seismic cloud.

5. Conclusions

The perforation-timing system has been developed to use the orientation shots (perforations, string shots, or other sources) for extracting appropriate compressional and shear wave velocities for ray paths traversing interwell sections. Since the orientation shots must be performed in all tests to orient receivers, their use for velocity measurements does not impact operations, yet they provide invaluable information on crosswell velocity structure. Since the measured ray paths are similar to those of the microseisms, this type of interrogation of the reservoir provides a more accurate and more realistic velocity interpretation than using dipole-sonic logs alone. However, dipole-sonic logs still provide the high-resolution structure that perforation timing measurements cannot provide and use of the interwell velocity analysis is typically to calibrate the dipole sonic log, if possible.

Perforation-timing velocities are often considerably different than those obtained from dipole-sonic logs. In some cases the velocities are less and in other cases the velocities are greater, and there are many cases where the two velocities have been found to be relatively similar. Where the velocities are different, the perforation-timing measurements have been found to yield more consistent microseismic locations.

Nothing in this study implies that the dipole-sonic logs are not accurate; rather, the velocities that are measured with the dipole-sonic log may not be representative of the velocities that control the microseismic radiation.

The determination of an accurate velocity structure is particularly important when the array is situated above the zone where microseisms are induced. Errors in both microseismic distance and elevation can be quite large in such cases. When the array straddles the microseismic zone, all location errors are reduced considerably, but the distance to events can still be significantly miscalculated if the correct velocities are not used. The effect of these errors can be important if there is a structure to the microseismic events that needs to be evaluated (e.g., a natural fracture system that is being activated). We have shown examples of unexpected interaction between hydraulic fractures and natural fractures. Fracture mapping is crucial for characterizing such treatments. In some cases the complex fractures yield a much better stimulation than traditional propped fractures.

6. References

Griffin, L.G., Sullivan, R., Wolhart, S., Waltman, C., Wright, C.A., Weijers, L., and Warpinski, N.R., “Hydraulic Fracture Mapping of the High-Temperature, High-Pressure Bossier Sands in East Texas,” SPE 84489, SPE Annual Technical Conference & Exhibition, Denver, Colorado, October 5 – 8, 2003.

Le Calvez, J.H., L. Bennett, K.V. Tanner, W.D. Grant, L.. Nutt, V. Jochen, W. Underhill, J. Drew, (2005), “Monitoring microseismic fracture development to optimize stimulation and production in aging fields“, Leading Edge, p. 72, January 2005.

Murphy, H.D. and M.C. Fehler, (1986), ”Hydraulic Fracturing of Jointed Formations”, SPE 14088.

Warpinski, N.R. , R.B. Sullivan, J. E. Uhl, C. K. Waltman, and S. R. Machovoe, (2003), “Improved Microseismic Fracture Mapping Using Perforation Timing Measurements for Velocity Calibration”, SPE 84488, 2003 SPE Annual Technical Conference and Exhibition held in Denver, Colorado, U.S.A., 5 – 8 October 2003.